HOKKAIDO UNIVERSITY

Title	HYDROGEN OVERVOLTAGE ON PLATINUM IN AQUEOUS SODIUM HYDROXIDE : Part Ⅰ. Rate of The Discharge Step
Author(s)	MATSUDA, A.; NOTOYA, R.
Citation	JOURNAL OF THE RESEARCH INSTITUTE FOR CATALYSIS HOKKAIDO UNIVERSITY, 14(2), 165-191
Issue Date	1966-12
Doc URL	https://hdl.handle.net/2115/24815
Type	departmental bulletin paper
File Information	14(2)_P165-191.pdf

Hokkaido University Collection of Scholarly and Academic Papers : HUSCAP

J. Res. Inst. Catalysis, Hokkaido Univ. Vol. 14, No. 2, pp. 165 to 191 (1966)

HYDROGEN OVERVOLTAGE ON PLATINUM IN AQUEOUS SODIUM HYDROXIDE

Part I. Rate of The Discharge Step

By

A. MATSUDA*) and R. NOTOYA*)

(Received September 12, 1966)

Abstract

Hydrogen overvoltage on Pt in aqueous NaOH and Na_2SO_4 was studied by means of the galvanostatic transient methods to distinguish the electrostatic part of the overvoltage from that due to the electronic work function of the electrode. The differential capacity of the electric double layer at the metal-solution interface and the rates of the electron transfer step were determined from the overvoltage-time curves at various values of pH and Na^+ concentration as a function of overvoltage. It was concluded that: 1) the electron transfer step is the discharge of Na^+, but not of a water molecule, and its rate obeys FRUMKIN's equation with the Tafel constant $\alpha=1/2$, 2) the exchange rate of the electron transfer step is proportional to the square root of Na^+ concentration and 10~100 times greater than that of the overall reaction, 3) the greater part of the overvoltage in steady states is attributed to the change in the work function of the electrode due to the formation of intermetallic compounds or solid solutions between Pt and Na produced by the discharge step.

Introduction

The hydrogen overvoltage is defined as the difference in the chemical potential of metal electron $\Delta\mu^e$ between the reversible and the irreversible states of the hydrogen electrode:

$$\eta = -\Delta\mu^e/F \qquad (1)$$

where μ^e is the chemical potential of metal electron and F the Faraday. The quantity η can be measured as the difference in the electrostatic potential between the lead wires of the same metal connected respectively to the reversible and the irreversible electrodes in the same environment. The chemical potential of metal electron is composed of the electrostatic potential φ and the

*) Research Institute for Catalysis, Hokkaido Univ., Sapporo, Japan.

electronic work function W of the metal as**)

$$\mu^e = -F(\varphi + W). \tag{2}$$

The hydrogen overvoltage is thus given by the difference in the electrostatic potential φ and that in the electronic work function W between the irreversible and the reversible states of the hydrogen electrode:

$$\eta = \Delta\varphi + \Delta W, \tag{3}$$

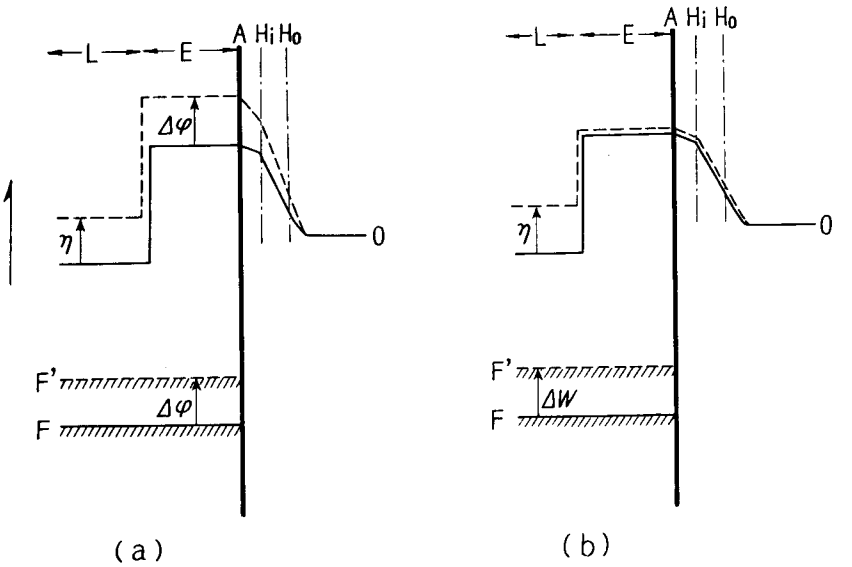

Fig. 1. Schematic diagrams of the distribution of the electrostatic potential and the FERMI level of an electrode when the surface is negatively charged. Full and dotted lines correspond respectively to the reversible and the irreversible states of the electrode reaction.

(a): the overvoltage is caused by the change in the potential difference across the metal-solution boundary, $\eta = \Delta\varphi$;

(b): the overvoltage is caused by the change in the work function of the electrode, $\eta = \Delta W$.

(η) overvoltage, (φ) cavity potential of the electrode referred to that inside the solution, (A) electrode surface, (E) electrode, (L) lead wire, (H_i) and (H_0) inner and outer HELMHOLTZ planes, (O) inside the solution, (F) or (F') FERMI level of electrons.

**) The term electrostatic potential in the present paper means the cavity potential indroduced by GRAHAME[1] which is defined as the potential of a point within a macroscopic cavity in a conductor. The work function is thus defined as the work necessary to take out an electron from interior of a conductor into a macroscopic cavity in the conductor.

The $\Delta\varphi$ is caused by charge up of the electric double layer at the metal-solution interface, while ΔW causes the change in the contact potential between the electrode and the lead wire, each of which alters readings of potentiometer, as illustrated in Fig. 1. The former depends on the structure of the double layer at the metal-solution interface and the latter on the electronic states of the electrode.

When the discharge step is rate-determining, the reaction rate has been derived as a function of $\Delta\varphi$ by FRUMKIN[2] in connection with the structure of the double layer at the metal-solution interface. In general case, however, neither the rate nor the species which discharges across the double layer has been separately determined because of experimental difficulties and in consequence no informations have been given on the intermediate species produced by the discharge step.

When the structural changes occur under the polarization due to intermediates produced by the discharge step or other elementary steps which compose the overall reaction, it is expected that the contact potential between the lead wire and the electrode or between the interior and the surface layers of the electrode methal itself plays an important role of determining the hydrogen overvoltage, as pointed out by LANGMUIR[3], since the work function of the electrode may be changed by the intermediates.

PAST and JOFA[4] have shown on the basis of the galvanostatic transient studies that the build up and decay of the hydrogen overvoltage on mercury can be attributed to $\Delta\varphi$ in the initial stages of the build up and the decay of the overvoltage. The galvanostatic transient methods also are applicable in solid hydrogen electrodes for determining $\Delta\varphi$ separately and further the rate of the discharge step as a function of $\Delta\varphi$ on the basis of informations on the differential capacity of the double layer, identifying the latter as the leak current of the double layer.

The aim of the present work is, on one hand, to determine the differential capacity of the double layer at the metal-solution interface and to find the rate of the discharge step as a function of $\Delta\varphi$ by the galvanostatic transient methods on the platinum hydrogen electrode in alkaline solutions containing sodium ions, and on the other hand, to elucidate the contribution of the change in the contact potential between the electrode and the lead wire to the hydrogen overvoltage due to the intermediates produced by the discharge step or other elementary steps in these solutions.

1. Theoretical treatments of the overvoltage-time curves

It will be discussed here how to find the differential capacity of the double

layer at the metal-solution interface and the rate of the discharge step from the overvoltage-time curves, which enable the change in the potential difference across the double layer to be distinguished.

When a constant polarizing current is applied to a hydrogen electrode, the overvoltage increases with time until it reaches a steady value and when the current is switched off, the overvoltage decreases first rapidly approaching zero asymptotically. We first consider the build up of overvoltage after switching on a current. On switching the current, the electrode surface is charged by the polarizing current to increase the electrostatic potential of the electrode. The discharge of the hydrogen electrode now proceeds to form intermediates on the electrode surface. The hydrogen overvoltage is thus caused first by charge up of the double layer at the metal-solution interface and then by the increase of intermediate as well. From the initial stage of the overvoltage-time curve where the hydrogen overvoltage can be regarded as due solely to charge up of the double layer, it is possible to determine the differential capacity of the double layer and the time constant of the discharge step on the basis of the theory of the galvanostatic transients developed by FRUMKIN *et al*[5]. A little different formula from that of FRUMKIN *et al* will be derived here for the analysis of the overvoltage-time curves in the region where the overvoltage increases due to charge up of the double layer at the metal-solution interface.

Electrons supplied by the polarizing current to the electrode are partly charged on the metal surface and partly consumed by the discharge reaction, *i.e.*, the leakage of the double layer. From the material balance of electrons within time interval δt, we have

$$\delta q = \delta q' - \delta q'' , \tag{4}$$

where δq, $\delta q'$ and $\delta q''$ are respectively an increment of electricity charged on the electrode surface, supplied by the polarizing current to the electrode and used for the discharge reaction. These quantities are respectively expressed as

$$\delta q = C_D \delta \varphi , \tag{5a}$$

$$\delta q' = -i \delta t , \tag{5b}$$

$$\delta q'' = -i_1 \delta t , \tag{5c}$$

where φ is the electrostatic potential of the electrode referred to that in the bulk of solution, C_D the differential capacity of the electric double layer at the metal-solution interface, i the polarizing current and i_1 the net rate of the discharge step expressed in terms of the electric current, the cathodic current being taken positive. Eiminating δq, $\delta q'$ and $\delta q''$ from Eqs. (4) and (5), we have

$$C_D = -(i-i_1)/\dot{\varphi}\,, \tag{6a}$$

or

$$i_1 = i + C_D\dot{\eta}\,, \tag{6b}$$

which enables i_1 to be evaluated when C_D is known in case where the variation of η consists practically in that of φ.

In the overvoltage region where $|\eta| \ll RT/F$, the rate of the discharge step is proportional to the overvoltage on the basis of the general theory of HORIUTI[6] admitted that the latter is the only irreversible step at the moment in question,

$$\eta = -r_1 i_1\,, \tag{7}$$

where

$$r_1 = RT/Fi_{10}\,, \tag{8}$$

is a constant in terms of the exchange current i_{10} of the discharge step. Eliminating i_1 from Eqs. (6b) and (7) and integrating, we have

$$\eta = r_1 i\left\{\exp(-t/\tau_1)-1\right\}\,, \tag{9}$$

where

$$\tau_1 = C_D r_1\,. \tag{10}$$

As seen from Eq. (9), τ_1 gives approximately a measure of time in which η attains $-r_1 i$ independent of the surface area of the electrode and is called the time constant of the discharge step. Differentiating Eq. (9) with time, we have

$$\ln(-i/\dot{\eta}) = t/\tau_1 + \ln C_D\,. \tag{11}$$

which states a linear relation between $\ln(-i/\dot{\eta})$ and t. The C_D and τ_1 can be experimentally evaluated from the latter linear relation, if observed at all at various current densities.

We consider now the decay process of the hydrogen overvoltage starting from a steady state by switching off the polarizing current. At the moment when the current is switched off, the overvoltage decays by decrease of electrons charged on the electrode surface through the discharge step with the rate equal to the polarizing current, since the concentration of the intermediate is kept constant at the moment. It follows that the differential capacity C_D of the double layer can be determined from the initial rate of the decrease of the overvoltage as

$$C_D = i/\dot{\eta}_{t=0}\,. \tag{12}$$

When the overvoltage thus decays exclusively by discharge of the double layer, the rate of the discharge step i_1 can be given by the following equation

$$i_1 = C_D\dot{\eta} \,. \tag{13}$$

Especially when the electrostatic component of the overvoltage in the steady state $\Delta\varphi$ is small as compared with RT/F, putting $\Delta\varphi=\eta_1$, we have similarly to the case of the build up

$$\eta_1 = -r_1 i_1 \,. \tag{14}$$

Eliminating i_1 from Eqs. (13) and (14) and putting $\dot{\eta}=\dot{\eta}_1$, we have

$$\eta_1 = -\tau_1\dot{\eta}_1 \,, \tag{15}$$

where $\tau_1=C_D r_1$ as in the case of build up. Integrating Eq. (15) with time and putting the initial condition $\eta_1=-r_1 i$ at $t=0$, we have

$$\eta_1 = -r_1 i \exp(-t/\tau_1) \,. \tag{16}$$

Differentiating Eq. (16) with time and putting $\dot{\eta}_1=\dot{\eta}$, we have similary to the case of build up

$$\ln(i/\dot{\eta}) = t/\tau_1 + \ln C_D \,, \tag{17}$$

C_D and τ_1 are determined by fitting Eq. (17) to the initial stage as functions of the overvoltage from which the decay curve starts.

The experimental results in the galvanostatic transient studies will be described in the following section on the platinum hydrogen electrode in alkaline solutions including sodium ions.

2. Experimental procedures

Special precaution was taken of the preparation of solutions and electrodes and of the purification of glass material used for the construction of cells against impurities, which are known to affect sensitively the hydrogen electrode reaction.

2.1. The reacton apparatus and preparation of solutions

Glass materials used for the reaction apparatus were preliminarily purified by steaming in a hydrogen stream for several hours after ordinary treatments of boiling in a mixture of concentrated nitric and sulfuric acids and washing with hot equilibrium water. Fig. 2 shows the reaction apparatus made of Halio glass (SHIBATA Co. Tokyo). Vessels 1~11 show the hydrogen purification train which is composed of cylinder hydrogen (1), trap (2), silica gel (3), hopkalite (4), soda lime (5), platinized asbestos (6), silica gel (7), trap (8), molecular sieve immersed in liquid nitrogen (9), liquid nitrogen traps (10) and (11). Silica gel and molecular sieve were preliminarily evacuated through stop cocks (A)

and (B) at temperatures 120 and 450°C respectively. Deionized water of specific resistance 10^7 Ω was introduced into vessel (a), and distilled with addition of potassium permanganate in a nitrogen stream into vessel (b) containing barium hydroxide, and then the water was distilled into flask (c), where the water thus distilled twice was boiled for several hours in a stream of purified hydrogen to remove traces of organic substances. The water thus purified was now ready for distillation into vessel (d) in which the solution of desired concentration was prepared as follows. Guaranteed reagent of sodium hydroxide or sodium sulfate (Koso Chemical Co. Tokyo) was introduced into vessel (d) through the intake (d_1) covered with a ground cap in a hydrogen stream and 150 cc of water purified in (c) was distilled into (d) in a stream of hydrogen. Then the solution thus prepared was transferred into pre-electrolysis cell (f) by hydrogen pressed in through greaseless stop cock (q_1) purging hydrogen in (f) through another greaseless stop cock (p_2). The solution was finally purified by pre-electrolysis in (f) between two electrodes of platinum foil with 20~30 mA/cm² for 30~50 hours. The solution thus purified was transferred into

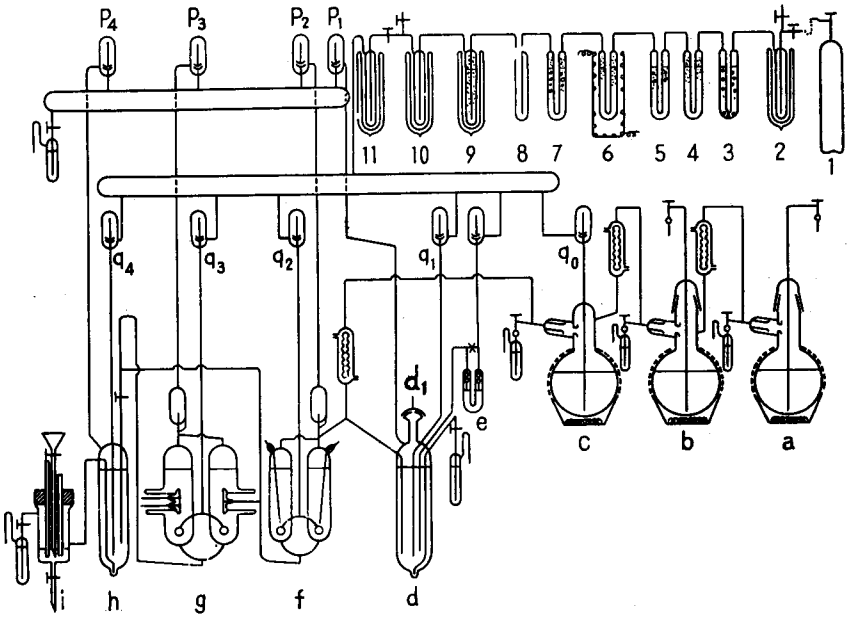

Fig. 2. The reaction apparatus.

(1)-(11) hydrogen purification train, (a)-(c) distillation apparatus of water, (d) solution vessel, (f) preelectrolysis cell, (g) cell including the test electrode, (h) solution storage vessel, (i) glass electrode for pH measurement, (d_1) ground glass cap, (e) purified SO_3 sealed in glass tube with breakable joints, (p_1)-(p_4), (q_0)-(q_4) greaseless valves for hydrogen path.

cell (g) containing the test electrode by hydrogen pressure. After each series of experiments in cell (g) the solution was transferred into vessel (h), a part of which being transferred into vessel (i) provided with a calomel and a glass electrode for the determination of pH of the solution.

2.2. Preparation of platinum film electrodes

The structure of the cell containing the test electrode is shown in Fig. 3(a), where (T), (R) and (A) are respectively the test, the reference and the counter electrodes. All electrodes are made of platinum films of ca. 1 μ thick which were prepared under vacuum of 10^{-6} mmHg by evaporating a platinum disk of purity 99.99% (JOHNSON MATTHEY) on a ground glass surface, heating the disk by means of an induction furnace at temperatures just below the melting

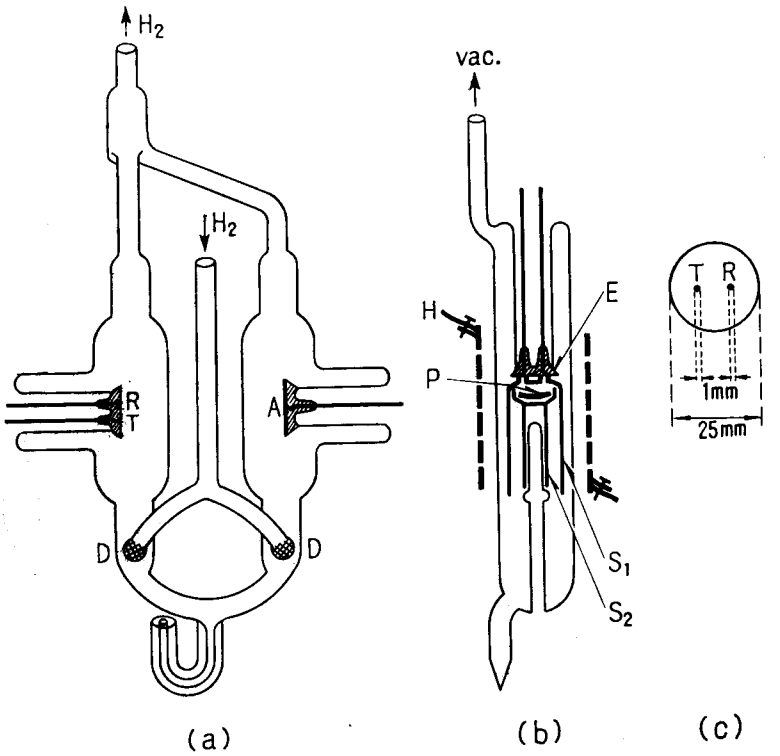

Fig. 3. Electrolytic cell (a), evaporation apparatus (b) and geometrical configuration of evaporated platinum film electrodes (c). (T), (R) and (A) test, reference and counter electrodes, (E) ground glass surface on which platinum is evaporated, (P) piece of platinum, (S_1) and (S_2) sample holder and cover made of quarz, (H) coil of induction furnace.

point of platinum, as shown in Fig. 3 (b). Fig. 3 (c) shows an example of the geometrical configuration of (T) and (R). Counter electrode (A) is 25 mm in diameter. The solution is stirred and circulated by hydrogen bubbles through glass filters (D).

Although platinum hydrogen electrodes thus prepared have high activities and rapid response, well reproducible results have been obtained in the galvanostatic transient measurements after repeated anodic polarizations for a few seconds at 1.8 v referred to the reversible hydrogen electrode.

2. 3. The electric circuit in the galvanostatic transient methods

The electric circuit is shown in Fig. 4. A polarizing current is supplied to cell (g) from 24 v battery through high resistance (R_1) and its strength is determined by measuring the potential drop across fixed resistance (R_2).

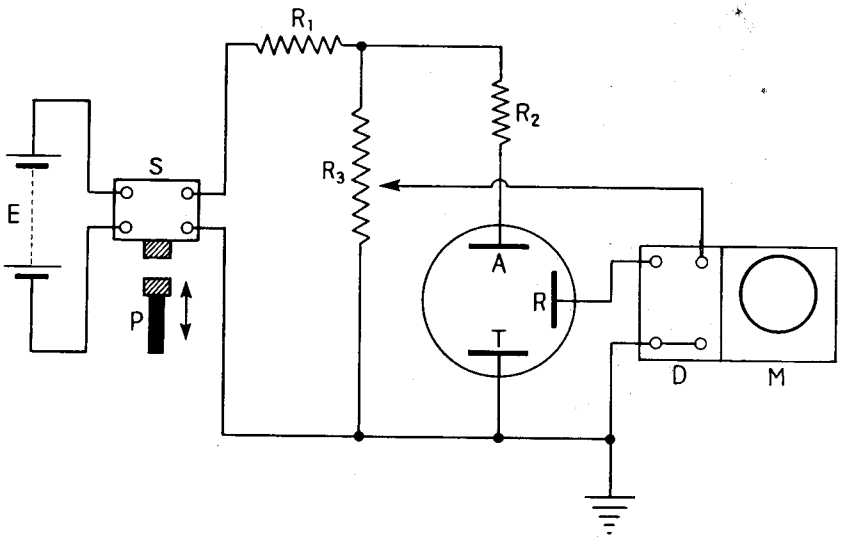

Fig. 4. The electric circuit for galvanostatic transient methods. (R_1), (R_2) and (R_3) resistances for current control, current measurement and compensation of ohmic overvoltage, (E) storage battery, (S) proximity switch, (D) high gain differential preamplifier, and (M) memoscope oscilloscope.

For the galvanostatic experiments it is desirable to switch a polarizing current in a shortest possible time, *e.g.*, within 1 μ sec. This can be achieved by the use of a proximity switch (TATEISH DENKI Co. Kyoto). The current is switched on by contact a piece of iron (P) with proximity switch (S) or off by separating (P) from (S). An example of the current-time relations is shown

in Plate I. Test and reference elctrodes (T) and (R) are connected respectively to terminals of a high gain differential preamplifier (D) attatched to a meoscope oscilloscope (M) (HUGH's Aircraft). The potential difference between (T) and (R) is observed on the memoscope screen. The ohmic potential drop between (T) and (R) caused by the resistance of solution can be separately determined from the oscillograms as the initial potential jump on switching on or off. This ohmic drop was compensated for expedient observations with a potential drop of reverse sign through resistance (R_3) imposed on terminals of (D) on switching.

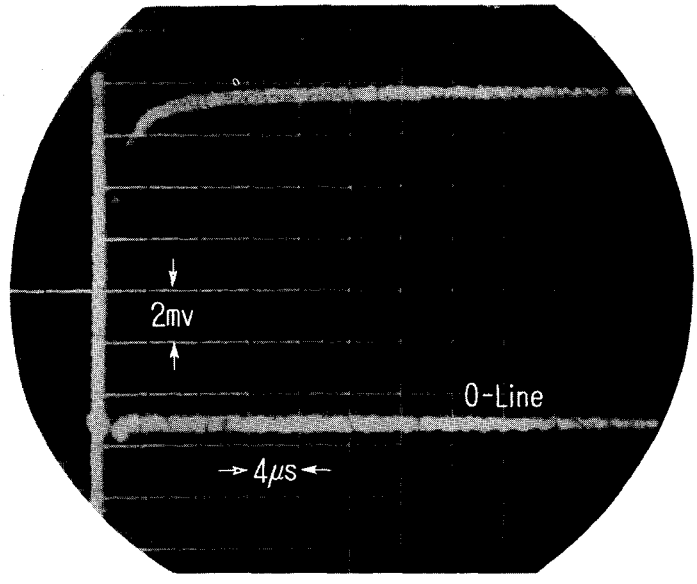

Plate 1. The current-time variation after switching on. The ordinate shows potential drop across R_2 (100 Ω), 2 mv/Division; the abscissa time after switching on, 4 μsec/Div.; solution 0.1 N $Na_2SO_{4,aq}$, pH 8.3.

3. Experimental results

The overvoltage-time curves after switching on or off the polarizing current have been observed in aqueous sodium hydroxide and sodium sulfate of various concentrations. Examples of the oscillograms are shown in Plates 2~11. As seen from the Plates, the potential difference due to the ohmic resistance of solutions can be clearly discriminated from the change in the true hydrogen overvoltage. From these oscillograms the rate of change in the overvoltage $\dot{\eta}$ is calculated at a given time after switching on or off the polarizing current, and the values of $\log(\mp i/\dot{\eta})$ are plotted against time in order to

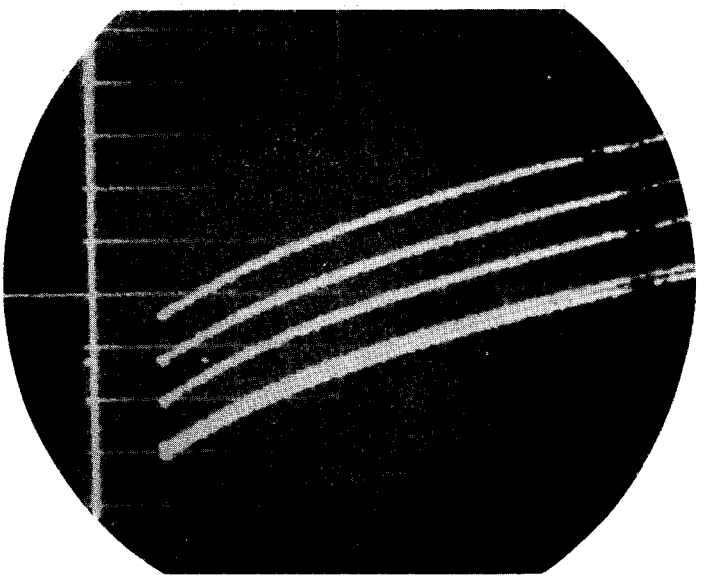

Plate 2. The potential-time variation after switching on a cathodic polarizing current on Pt in 0.1 N $NaOH_{aq}$, $i = 6.1 \cdot 10^{-4}$ amp.,1 mv/Div, 20 μs/Div.

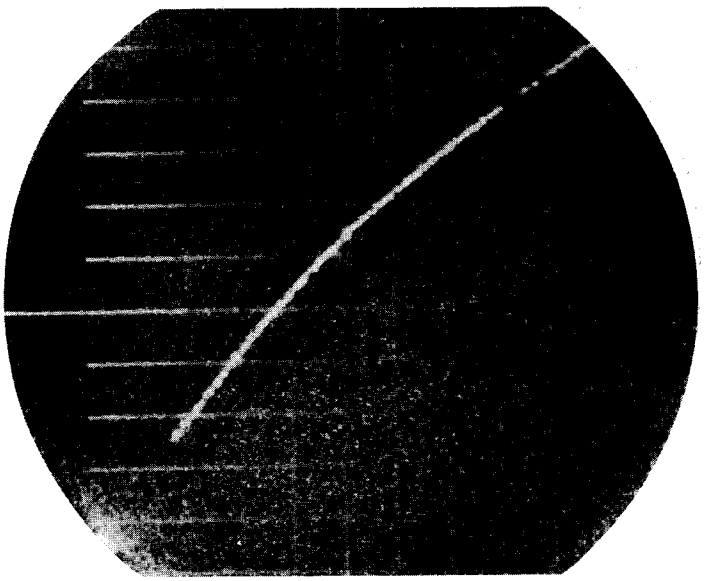

Plate 3. The potential-time variation after switching on a cathodic polarizing current on Pt in 0.1 N $NaOH_{aq}$, $i = 4.6 \cdot 10^{-3}$ amp, 2 mv/Div, 10 μs/Div.

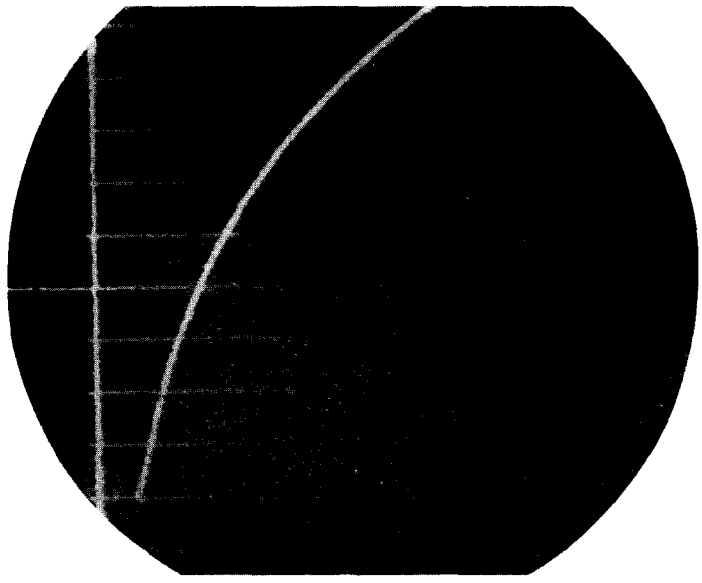

Plate 4. The potential-time variation after switching on a cathodic polarizing current on Pt in 0.1 N $NaOH_{aq}$, $i=4.6\cdot10^{-3}$ amp., 10 mv/Div, 100 μs/Div.

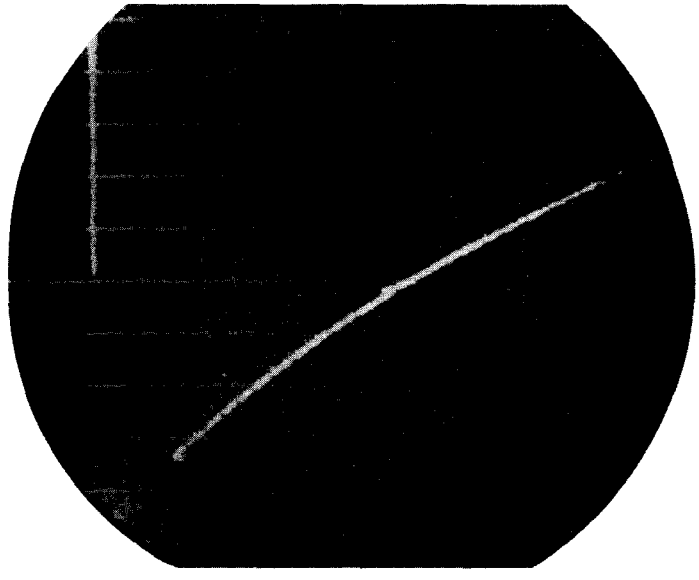

Plate 5. The potential-time variation after switching on a cathodic polarizing current on Pt in 0.1 N $NaOH_{aq}$, $i=8.4\cdot10^{-3}$ amp., 5 mv/Div, 10 μs/Div.

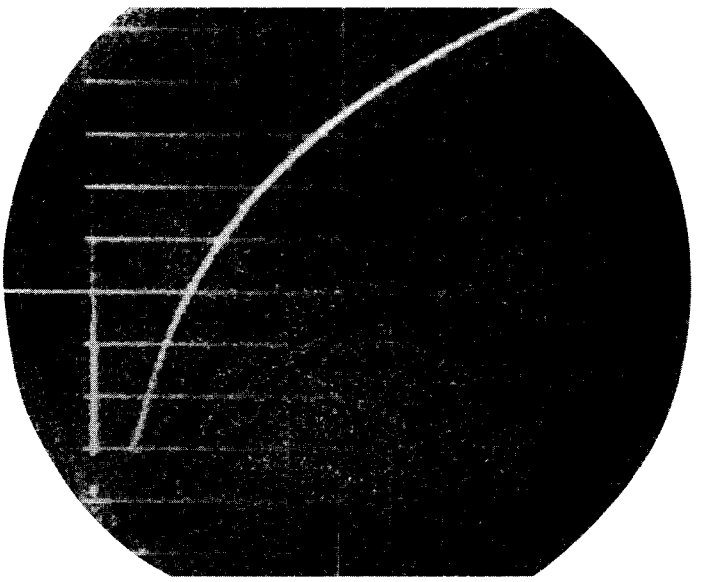

Plate 6. The potential-time variation after switching on a cathodic polarizing current on Pt in 0.1 N $NaOH_{aq}$, $i = 8.4 \cdot 10^{-3}$ amp., 10 mv/Div, 100 μs/Div.

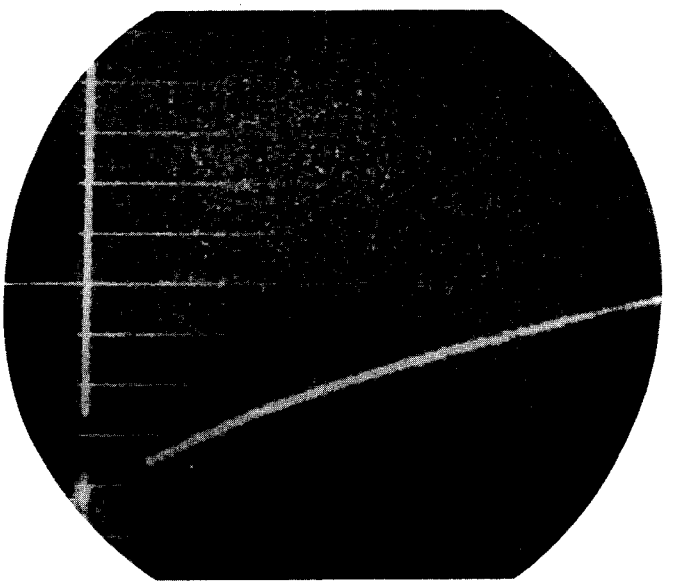

Plate 7. The potential-time variation after switching on an anodic polarizing current on Pt in 0.1 N $NaOH_{aq}$, $i = 6.1 \cdot 1010^{-4}$ amp., 1 mv/Div, 20 μs/Div.

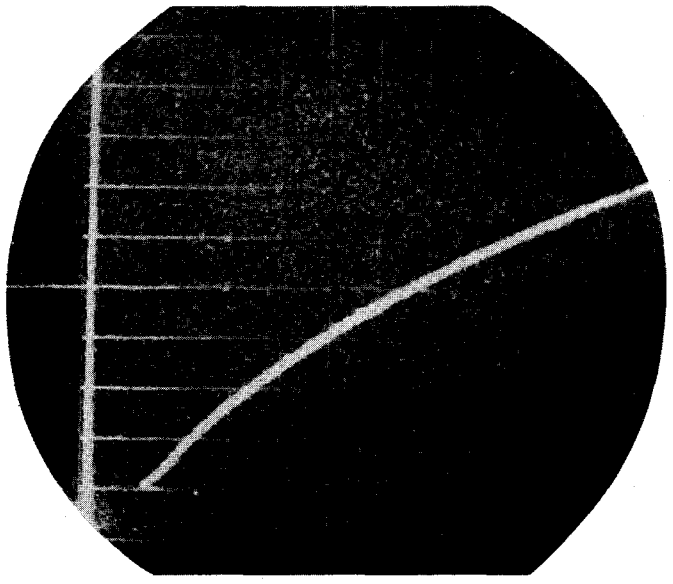

Plate 8. The potential-time variation after switching on an anodic polarizing current on Pt in 0.1 N $NaOH_{aq}$, $i=6.1\cdot10^{-4}$ amp., 1 mv/Div, 50 μs/Div.

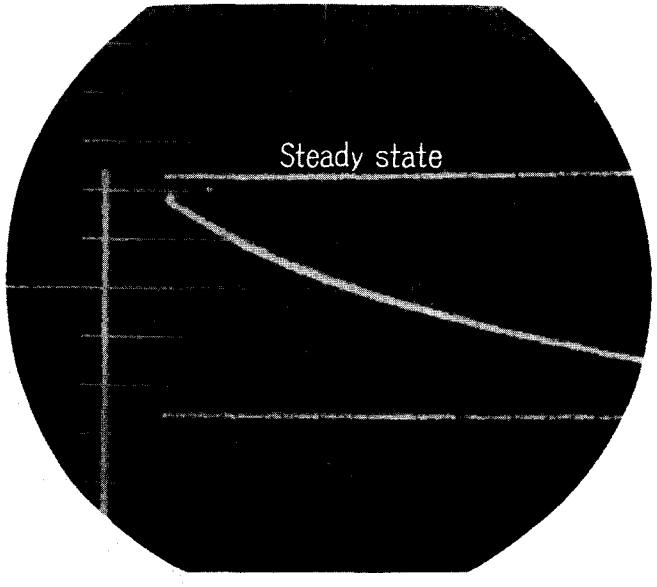

Plate 9. The potential-time variation after switching off a cathodic polarizing current on Pt in 0.1 N $NaOH_{aq}$, $i=1.4\cdot10^{-3}$ amp., 2 mv/Div, 20 μs/Div.

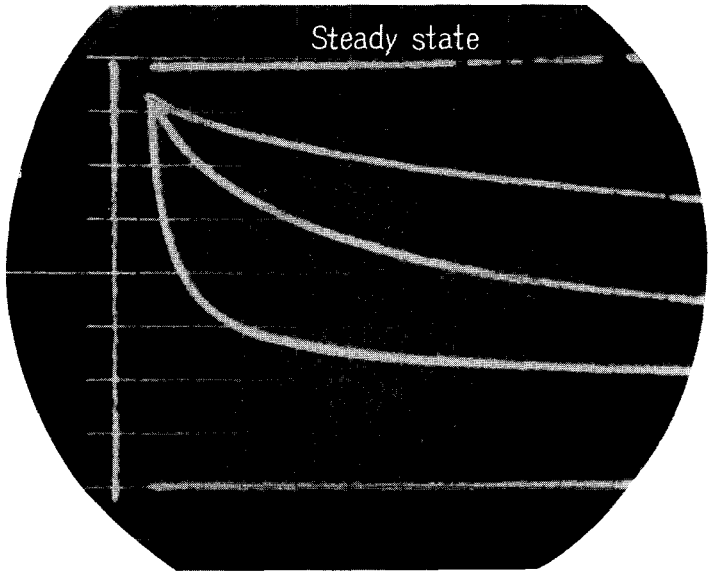

Plate 10. The potential-time variation after switching off a cathodic polarizing current on Pt in 0.1 N $NaOH_{aq}$, $i=1.4\cdot10^{-3}$ 10 amp., 10 mv/Div., 100, 200, 500 μs/Div.

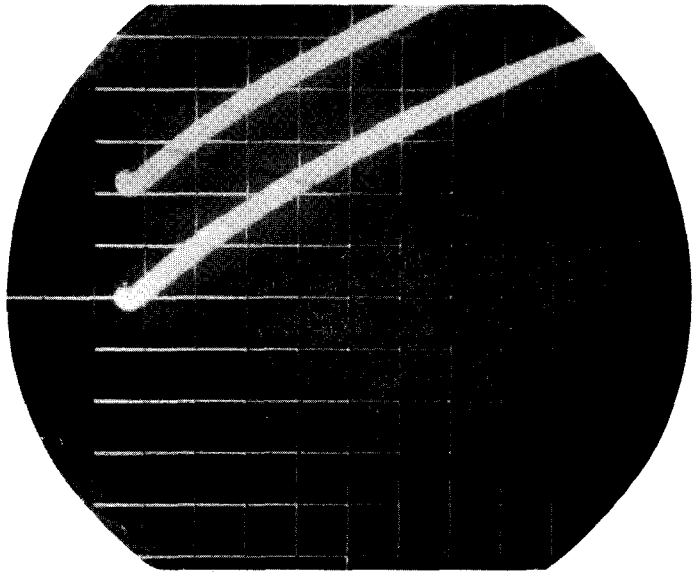

Plate 11. The potential-time variation after switching on a polarizing current on Pt in aqueous 0.1 N Na_2SO_4, pH 8.3, $i=1\cdot10^{-3}$ mp., 1 mv/Div, 10 μsec/Div.

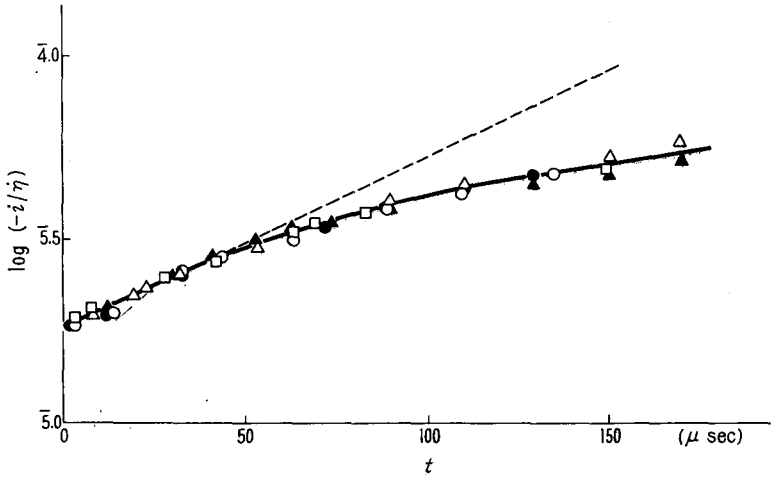

Fig. 5. The relation between $\log(-i/\dot{\eta})$ and time after switching on the cathodic polarizing current on an evaporated platinum film in $NaOH_{aq}$, pH 13.0; the apparent area 0.13 cm^2; the polarizing currents i (amp): (○) $6.1\cdot10^{-4}$, (●) $1.19\cdot10^{-3}$, (△) $2.7\cdot10^{-3}$, (▲) $4.9\cdot10^{-3}$, (□) $8.4\cdot10^{-3}$; $C_D=17.5$ μF, $\tau_1=92.4$ μsec.

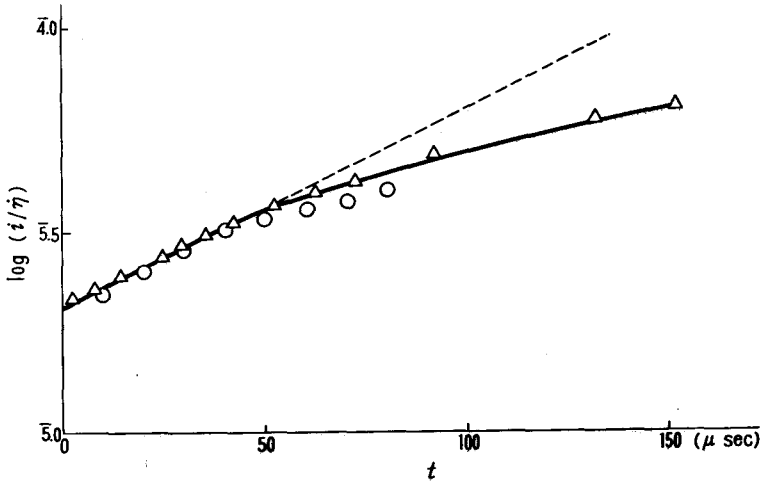

Fig. 6. The relation between $\log(i/\dot{\eta})$ and time after switching off the cathodic polarizing current, the electrode and the solution are the same as in Fig. 6; the current i and the starting overvoltage η_s: (○) $1.4\cdot10^{-3}$ amp. and $\eta_s=-50$ mv, (△) $8.9\cdot10^{-3}$ amp. and $\eta_s=-106$ mv; $C_D=20.4$ μF and $\tau_1=87$ μsec.

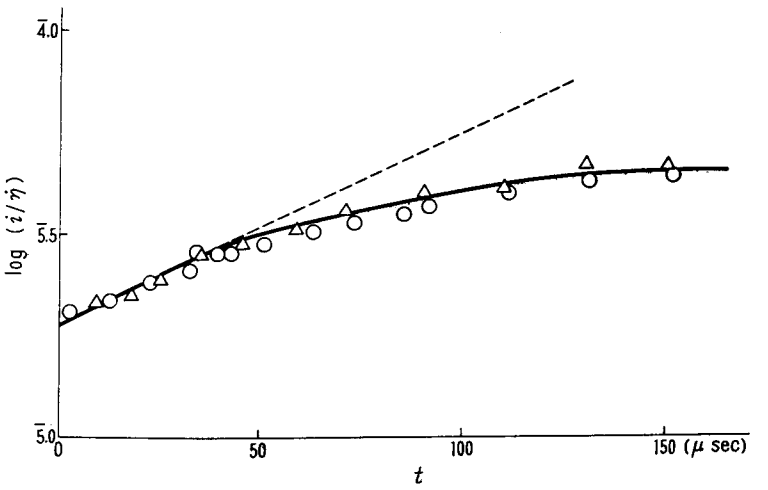

Fig. 7. The relation between $\log(i/\dot{\eta})$ and time after switching on the anodic polarizing current, the electrode and the solution are the same as in Fig. 6; the currents i; (○) $1.19\cdot10^{-3}$ amp., (△) $2.73\cdot10^{-4}$ amp; $C_D=18.1\ \mu$F and $\tau_1=91.4\ \mu$sec.

put Eqs. (7) and (13) to the test. Examples of the relation between $\log(\mp i/\dot{\eta})$ and time are illustrated in Figs. 5~11. These Figures show the linear relation between $\log(\mp i/\dot{\eta})$ and time every magnitude of polarizing current and every solution used in the present experiment valid at the initial stages of the build up and decay curves throughout. C_D and τ_1 evaluated from these Figures according to Eqs. (7) and (13) are now examined whether they satisfy the necessary conditions for being the differential capacities and the time constants of the discharge step of the hydrogen electrode reaction respectively; the necessary condition for C_D is its constancy for an electrode of constant surface area, and that for τ_1 is its independence of the electrode area, which are checked in the following sections in a) and b) respectively, and on which basis the rate of the discharge step is formulated in c).

a) The differential capacity of the electric double layer

The relations between $\log(\mp i/\dot{\eta})$ and time are shown in Figs. 5, 6, 7 and 8(b) as derived from the overvoltage-time curves observed with an evaporated film of apparent area 0.13 cm^2 in $NaOH_{aq}$, pH 13.0 and in 0.1 N Na_2SO_4, pH 11.0. The value of C_D is found to be constant at 18 μF independent of pH within experimental errors or of the direction of polarization, as seen from comparison of Fig. 5 and 7. The same value of C_D is also obtained from

decay curves starting from -50 and -106 mv, as seen from Fig. 6. Comparing Figs. 5 and 8(b), it is found that C_D remains constant as the electrolyte varies from NaOH to Na_2SO_4. The constant value of C_D is thus secured from the $\log(\mp i/\dot{\eta})\sim t$ relations throughout every solution and polarization examined on one and the same electrode.

Figs. 8(a) and 9 show the relation between $\log(-i/\dot{\eta})$ and time in sodium sulfate observed with an evaporated film of apparent area 0.07 cm^2. The value of C_D is found 11 μF.

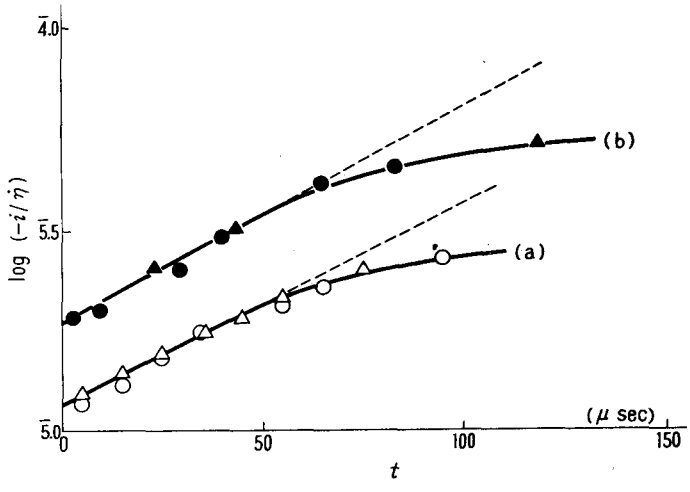

Fig. 8. The relation between $\log(-i/\dot{\eta})$ and time in the build up processes on platinum in 0.1 N Na_2SO_4. (a): apparent area 0,07 cm^2, pH 8.3 and the currents (○) $4.7\cdot10^{-4}$ amp, (△) $1.0\cdot10^{-3}$ amp; $C_D=11$ μF and $\tau_1=90$ μsec. (b): apparent area 0.13 cm^2, pH 11.0 and the currents (●) $5.25\cdot10^{-4}$ amp, (▲) $2.25\cdot10^{-4}$ amp; $C_D=18$ μF and $\tau_1=84$ μsec.

The overvoltage-time curves were observed further on two platinum films of different area evaporated at the same time on different parts of one and the same ground glass surface, using a quarz cap with two openings in the evaporation apparatus in Fig. 3(b). The $\log(-i/\dot{\eta})\sim t$ relations on these electrodes in $NaOH_{aq}$ of pH 13.45 and 11.9 are shown respectively in Figs. 10 and 11. As seen from these Figures, a constant definite value of C_D is obtained on each electrode, while the values of C_D of the two electrodes are proportional to their apparent area. The proportionality of C_D to the apparent area for platinum film electrodes prepared under the same conditions of evaporation has been generally established, as shown in Fig. 12. It is concluded from these

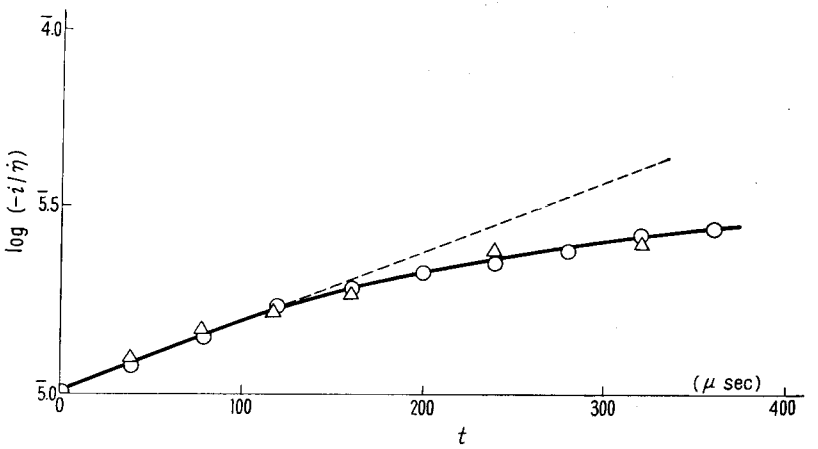

Fig. 9. The relation between $\log(-i/\dot{\eta})$ and time in the build up processes on platinum in 0.01 N Na_2SO_4, pH 8.2, apparent area 0.07 cm², the currents (○) $2.3\cdot10^{-4}$ amp, (△) $3.4\cdot10^{-4}$ amp; $C_D=10\mu$F and $\tau_1=246$ μsec.

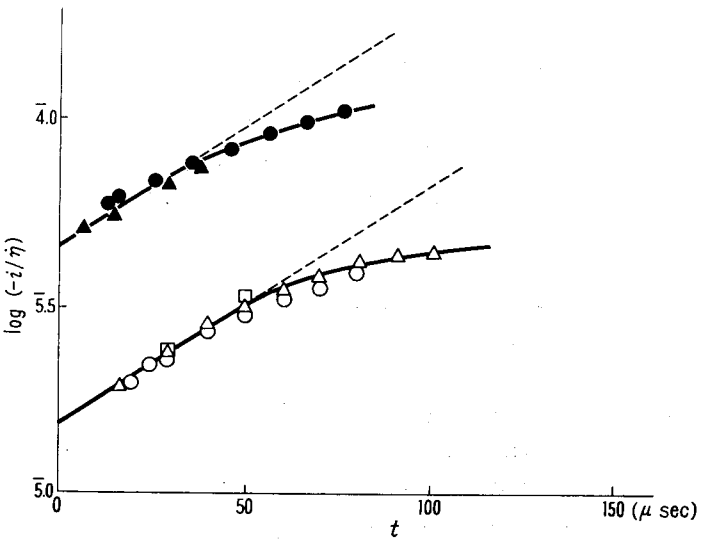

Fig. 10. The relation between $\log(-i/\dot{\eta})$ and time in the build up processes on evaporated platinum films, apparent area 0.1 and 0.3 cm², in $NaOH_{aq}$ pH 13.45; the currents (○) $1.15\cdot10^{-3}$ amp, (△) $2.25\cdot10^{-3}$ amp, (□) $3.9\cdot10^{-5}$ amp, (▲) $2.9\cdot10^{-3}$ amp; $C_D=15$ and 46 μF respectively and $\tau_1=73$ μsec.

experimental results that C_D determined from the linear relations between log $(\mp i/\dot{\eta})$ and time satisfies the necessary condition mentioned in the foregoing section, of being the differential capacities of the electric double layers at the metal solution interfaces.

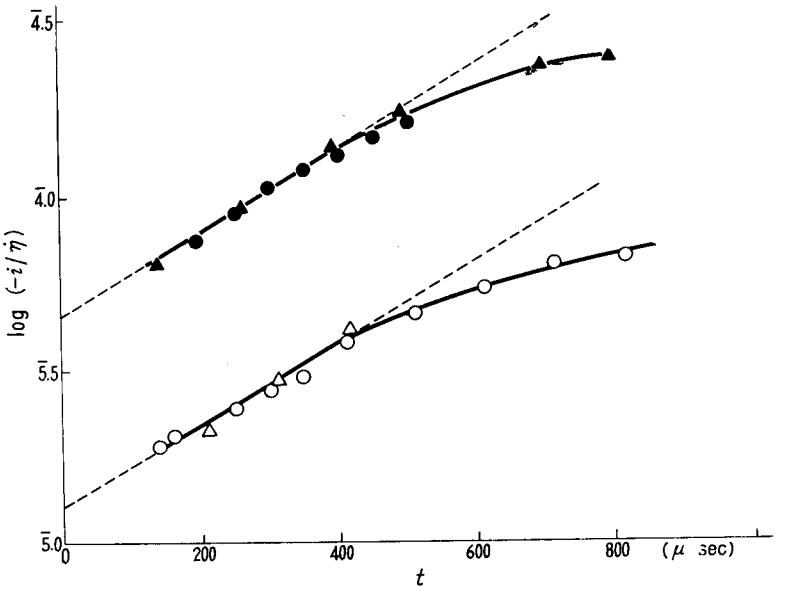

Fig. 11. The relation between log $(-i/\dot{\eta})$ and time in the build up processes in $NaOH_{aq}$, pH 11.9, the electrodes are the same as in Fig. 10; the currents (○) (●) $2.23 \cdot 10^{-4}$ amp, (△) (▲) $4.06 \cdot 10^{-4}$ amp; $C^D = 13$ and 44 μF respectively and $\tau_1 = 326$ μsec.

b) The time constant of the discharge step

It is assumed that the overvoltage is that due to charge up of the double layer at the metal-solution interface in the overvoltage region where log $(\mp i/\dot{\eta})$ varies linearly with time, inasmuch as C_D obtained from the extraporation of this linear part satisfies the condition of being the differential capacity of the double layer as described in a). The τ_1's obtained from these linear relations are then the time constants of the discharge step in accordance with Eq. (11) or (17). The values of τ_1 thus determined are now commented upon in what follows.

First, Figs. 10 and 11 show that τ_1 is independent of the electrode area, satisfying the condition that τ_1 is the time constant of the discharge step. Figs. 5, 10 and 11 indicate on the other hand that τ_1 obtained from the build up

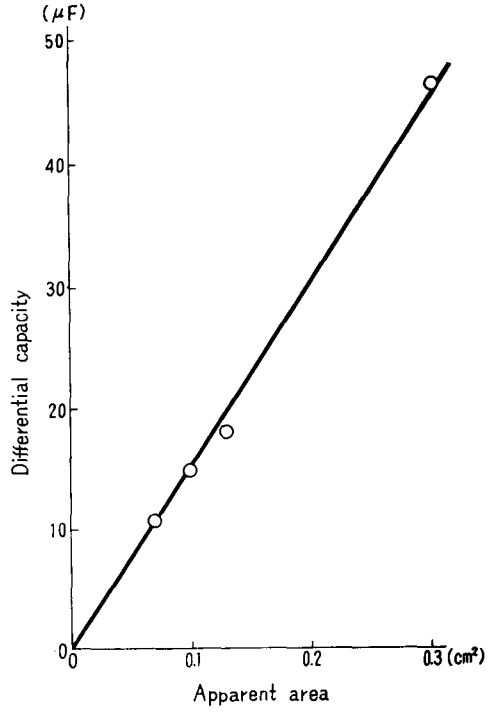

Fig. 12. The relation between the differential capacities of the electric double layer and the apparent area of evaporated platinum films in $NaOH_{aq}$.

curves in $NaOH_{aq}$ increases with decrease of pH. Comparison of Figs. 5 and 6 reveals that τ_1 obtained from the decay curves coincides with that obtained from the build up curves in the same solution, *i.e.*, τ_1 is constant independent of the overvoltage. Figs. 8 and 9 show, on the other hand, that τ_1 in Na_2SO_4 does not depend on pH, but on the concentration of sodium ion C^{Na^+}.

The τ_1's obtained in various solutions are tabulated in Table I and $\log \tau_1$ is plotted against pH or $\log C^{Na^+}$ in Fig. 13. As readily seen from the Figure, the $\log \tau_1$ varies linearly with $\log C^{Na^+}$ with gradient $-1/2$ independent of pH and irrespective as to whether τ_1 is derived from the build up or the decay curves. It follows that the exchange current of the discharge step i_{10} is proportional to the square root of C^{Na^+},

$$i_{10} = k(C^{Na^+})^{1/2}, \tag{18}$$

since i_{10} is related to τ_1 by Eqs. (8) and (10) as

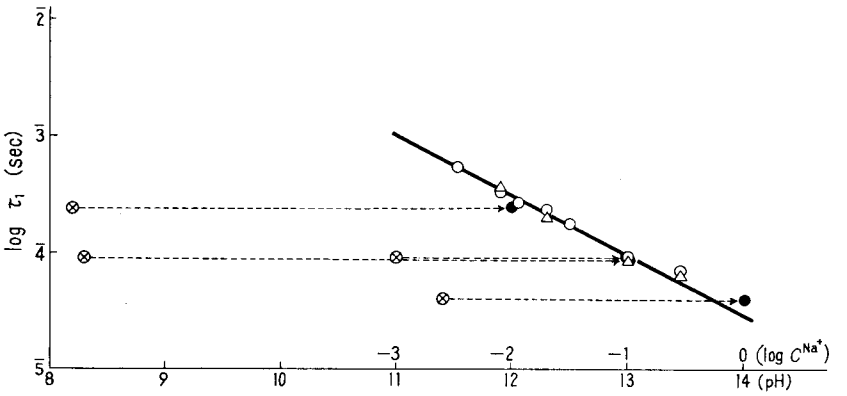

Fig. 13. The relation between $\log \tau_1$ and pH or $\log C_{Na^+}$. (○) from build up burves in $NaOH_{aq}$; (⊗) or (●) from build up curves in aqueous Na_2SO_4 plotted against pH or $\log C^{Na^+}$; (△) from decay curves in $NaOH_{aq}$.

TABLE I. Kinetic parameters of the discharge step of platinum hydrogen electrode reaction in alkaline solutions containing sodium ions

Electrolyte	pH	C^{Na^+} (N)	Build up		Decay		
			τ (μ sec)	i_{10} (amp/cm²)	τ_1 (μ sec)	i_{10} (amp/cm²)	$-\eta_s$ (mv)
NaOH	13.45		72.5	$6.20\cdot10^{-3}$	70	$6.42\cdot10^{-3}$	80
〃	13.00		92.4	4.86 〃	87	5.16 〃	106, 50
〃	12.50		175	2.57 〃			
〃	12.30		235	1.91 〃	203	2.22 〃	48
〃	12.03		265	1.70 〃			
〃	11.90		326	1.38 〃	352	1.28 〃	40, 70
〃	11.53		530	0.85 〃			
Na_2SO_4	8.20	0.01	246	1.83 〃			
〃	8.30	0.1	90	5.0 〃			
〃	11.00	0.1	84	5.35 〃			
〃	11.38	1.0	42	10.7 〃			

Note: the exchange current of the overall reaction $i_0=3.1\cdot10^{-4}$ amp/cm².

$$i_{10} = C_D RT/F\tau_1 . \tag{19}$$

It may be concluded from these results that the discharge step of the hydrogen

electrode reaction in these solutions is not the discharge of a water molecule as usually accepted[7], but the discharge of a sodium ion. On the other hand, the exponent of C^{Na^+} in Eq. (18) can be identified with the TAFEL constant of the discharge reaction on the basis of the FRUMKIN's theory[5], so that it may be valid to assume that the rate of the discharge step can be expressed as

$$i_1 = k(C^{Na^+})^{1/2}\left\{\exp(-F\eta_1/2RT) - \exp(F\eta_1/2RT)\right\}, \qquad (20)$$

where η_1 denotes $\Delta\varphi$ or the overvoltage of the discharge step.

c) The rate of the discharge step

The rate of the discharge step i_1 can be calculated by Eq. (6 b) from i, C_D and $\dot{\eta}$ relevant to the overvoltage curve. The relations between i_1 and η thus calculated from the build up curves in aqueous NaOH of pH 13.0 and 13.3

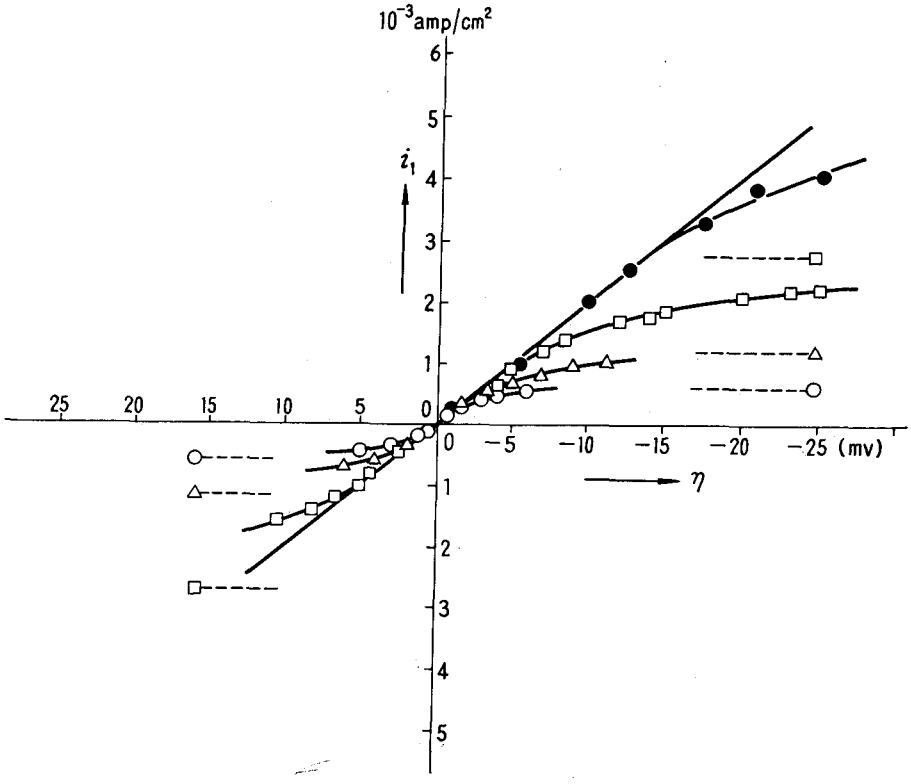

Fig. 14. The relation between the current density of the discharge step and the overvoltage in $NaOH_{aq}$, pH 13.0, in the build up processes; the polarizing current (○) $6.1\cdot10^{-4}$ amp/cm² (△) $1.19\cdot10^{-3}$ amp/cm² (□) $2.73\cdot10^{-3}$ amp/cm² (●) $8.4\cdot10^{-3}$ amp/cm².

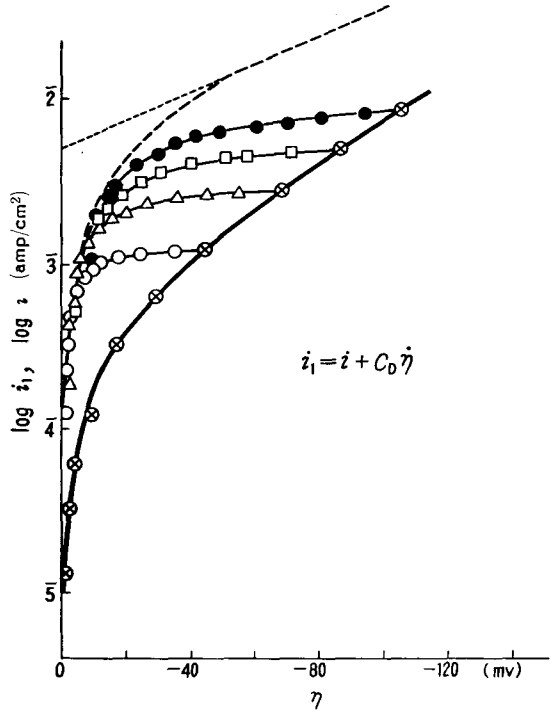

Fig. 15. The relation between $\log i_1$ *vs.* η in the build up processes, and $\log i$ *vs.* η in steady states in $NaOH_{aq}$, pH 13.0; the polarizing current (○) $1.2\cdot10^{-3}$ amp/cm², (△) $2.7\cdot10^{-3}$ amp/cm², (□) $4.8\cdot10^{-3}$ amp/cm², (●) $8.3\cdot10^{-3}$ amp/cm²; (⊗) denotes $\log i$ *vs.* η in steady states.
The broken line shows $\log i_1$ *vs.* η calculated by the FRUMKIN's equation using i_{10} obtained from τ_1.

are respectively shown in Figs. 14, 15 and 16.

It is seen from Fig. 14 that i_1 is proportional to η in the overvoltage region where $|\eta| \ll RT/F$. The proportionality constant $r_1 = -\eta/i_1$ is found $5\Omega\cdot cm^2$ which coincides with that calculated from C_D and τ_1 determined from $\log(-i/\dot{\eta}) \sim t$ relation in Figs. 5*). Fig. 15 and 16 show the $\log i_1 \sim \eta$ relations in the whole region of the overvoltage in the build up processes. We see from these Figures that the discharge step nearly attains its steady state with very small value of η or at the initial stage of the build up process, and that the $\log i_1 \sim \eta$ curves coincide with the theoretical one calculated by Eq. (20)

*) P. DOLIN, B. ERSHLER and A. FRUMKIN[8] have early obtained the value of r_1 $5\Omega\cdot cm^2$ in N $NaOH_{aq}$ by means of the conductivity measurements using alternating current at a frequency 375 c.p.s.

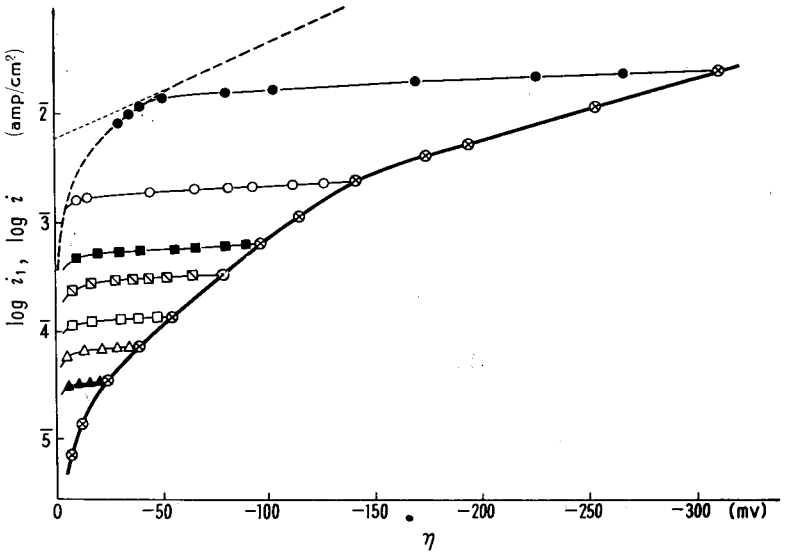

Fig. 16. The relation between $\log i_1$ and η in the build up processes, and $\log i$ and η in steady states on a less active platinum film electrode in $NaOH_{aq}$, pH 13.3. The broken line shows $\log i_1$ *vs.* η calculated by the FRUMKIN's equation using i_{10} obtained from τ_1, and (⊗) shows $\log i$ *vs.* η in steady states.

using i_{10} derived from τ_1 and C_D in the initial stages of the build up processes. These facts show that the increase of the overvoltage cannot be exclusively attributed to the increase of $\Delta\varphi$.

4. Discussions

As described in the introduction, the overvoltage is composed of $\Delta\varphi$ and ΔW, *i.e.*, the change in the potential difference across the double layer at the metal-solution interface and that in the contact potential between the electrode and the lead wire.

It has been experimentally found that there exists a linear relation between $\log(\mp i/\dot{\eta})$ and time in the initial stage of the build up and decay curves and C_D determined from this linear relation on the basis of Eq. (11) or (17) is identifiable with the differential capacity of the electric double layer at the metal-solution interface. It can be concluded from these results that the increase of the overvoltage can be attributed exclusively to $\Delta\varphi$ in this initial stage. It has further been found that C_D thus determined is constant independent of η and the rate i_1 of the discharge step calculated by equation $i_1 = i + C_D\dot{\eta}$ on the basis of constancy of C_D obeys the following equation in the initial stage within

time interval τ_1 for every build up curve observed

$$i_1 = i_{10}\left\{\exp(-\Delta\varphi/2RT) - \exp \Delta\varphi/2RT)\right\}, \qquad (20)$$

where i_{10} is calculated from τ_1 and C_D by Eq. (19). This equation corresponds to FRAMKIN's equation simplified neglecting Ψ_1-potential on the HELMHOLTZ plane in the double layer[5].

If the $\log i_1 \sim \eta$ curves coincide with the $\log i \sim \eta$ in steady states throughout the build up of the overvoltage, the discharge step may be regarded as rate-determining. It has been found, however, that the $\log i_1 \sim \eta$ relation deviates definitely from $\log i \sim \eta$ relation, as illustrated in Figs. 15 and 16, practically $\log i_1$ being hept constant after the lapse of time interval τ_1 and consequently the discharge step is excluded from being rate-determining.

We discuss here the increase of the overvoltage in the later stages of the build up curves after the lapse of time interval τ_1. In this later stage the increase of the overevoltage cannot exclusively be attributed to $\Delta\varphi$, since if it were so, i_1 should increase far beyond i with increase of the overvoltage according to Eq. (20) contrary to the experimental results, as seen from Figs. 15 and 16. The discharge step can be regarded as nearly in steady state in this later stage, since τ_1 measures the time in which the discharge step attains its steady state after switching on the polarizing current, as seen from Eq. (9). It is thus suggested that the charge density on the electrode surface is nearly kept constant and in consequence $\Delta\varphi$ remains constant with increase of η in this later stage, inasmuch as C_D is constant independent of η as stressed in the foregoing section. It is thus assumed that the increase of η is attributed to ΔW in this later stage of the build up curves, which can be expected by the structural change of the electrode due to the formation of an intermetallic compound or a solid solution between platinum and sodium atom produced by the discharge step, as mentioned in the foregoing section.

The rate-determining step and the intermediates of the hydrogen electrode reaction will be discussed in the following papers.

Conclusive remarks

The platinum hydrogen electrode in aqueous NaOH and Na_2SO_4 has been studied by means of the galvanostatic transient methods.

It has been found that the discharge step is the discharge of sodium ion and its rate obeys FRUMKIN's equation simplified neglecting the Ψ_1-potential on the HELMHOLTZ plane in the double layer and further suggested that the work function of the electrode is changed by the initermediate sodium atom produced by the discharge step.

Acknowledgement

The authors wish to express their sincere thanks to Prof. Emeritus J. HORIUTI for his helpful discussions on the present work, and also their deep gratitude to Prof. A. N. FRUMKIN and to prof. L. I. Antropov for their kind advices on the prsent work.

References

1) D. C. GRAHAME, Chem. Rev., **41**, 441 (1947).
2) A. FRUMKIN, Z. physik. Chem., **A 164**, 121 (1933).
3) I. LANGMUIR, Trans. Amer. Electrochem. Soc., **29**, 125 (1916).
4) V. E. PAST a. Z. A. JOFA, J. Phys. Chem., U.S.S.R., **33**, 913 (1959).
5) A. N. FRUMKIN, V. S. BAGOTSKY, Z. A. JOFA a. B. N. KABANOV, "*Kinetics of Electrode Processes*", Moscow University Press, P. 151 (1952).
6) J. HORIUTI, *this Journal*, **5**, 1 (1957).
7) A. N. FRUMKIN, *Advances in Electrochemistry and Electrochemical Engineering*, Vol. Edited by P. DELAHAY, Interscience Publishers, New York, London, P. 65 (1961).
8) P. DOLIN, B. ERSHLER a. A. FRUMKIN, Acta Physicochim. U.R.S.S., **13**, 779 (1940).